Selective Hydrogenation of Acetylene through a Short Contact Time Reactor

Matthew J. Vincent and Richard D. Gonzalez
Dept. of Chemical Engineering, Tulane University, New Orleans, LA 70118

A novel approach to the selective hydrogenation of acetylene involves a short contact time reactor. A thin Pd/γ-Al_2O_3 catalytic membrane (about 5 μm thick) was observed to be void of minor defects. Forcing a dilute $C_2H_2/H_2/Ar$ mixture through the layer produced high conversions coupled with high selectivity at high temperatures. The selectivity was observed to increase with temperature. A gas-dispersion model with derived kinetics was employed to explain the results. A solution to the corresponding coupled nonlinear differential equations resulted in a Peclet number of 64.5 and a contact time of 9.5×10^{-3} s through the reactor at 100°C. A critical thickness is predicted to exist for a maximum in ethylene concentration. A value of 2.5 μm at 200°C is representative. Lastly, permeability experiments agree with modeling results to show that Knudsen diffusion is absent despite a narrow pore-size distribution.

Introduction

The selective hydrogenation of acetylene has been important to the polyethylene industry since the 1960s. Today it contributes to over 45% of the plastic market or about $55 billion (Weirauch, 2000). Although the weight fraction of acetylene is only about 0.35% of the feedstock, it must be reduced to between 5 and 10 ppm (99.97% conversion) to prevent undesirable properties in polyethylene. The removal of acetylene can be achieved by either reaction and/or separation. Acetylene can be separated by liquifaction, but its compression is both dangerous and expensive. The selective hydrogenation of acetylene in a catalytic bed is less expensive and yields more ethylene for polyethylene production. Metals that have a high activity for hydrogenation reactions include Rh, Ru, Pd, Pt, and Ni (Benner et al., 1991). However, Pd is unique in its ability to selectively hydrogenate alkynes and dienes in the presence of alkenes (Gates et al., 1979) and was shown by Bond (1963) to be the most selective metal. In an industrial reactor, Pd is either impregnated or ion-exchanged on an α-Al_2O_3 pellet to yield a low surface area (20 m^2/g), high dispersion catalyst with a low palladium loading (0.04 wt. %; from Lam and Lloyd, 1972). With an excess of ethylene, the low loading is thought to inhibit the readsorption of ethylene for a further reaction.

Understandably, too much of the ethylene feed stock is consumed by direct hydrogenation. Many authors have attempted to improve the fundamental understanding of the process and have developed novel approaches to selective hydrogenations. One approach is to use a membrane reactor (Armor, 1995). It may be either a supported ceramic layer on a porous support or an ultrathin solid noble metal. Some metal membrane studies include Pd/Ni (Gryaznov et al., 1981) and Pd, Pd/Ni, Pd/Ru, and Pd/Ag (Itoh et al., 1993). Both studies found that the permeate hydrogen was very active and that ethylene was the main product. However, they must be very thin in order to provide the appropriate selectivity.

Porous ceramic membranes can support highly dispersed metals on an inorganic oxide to combine the properties of higher permeability with thermal stability, which are absent in the dense metal membranes. In addition, ceramic substrates provide for a smaller pressure drop at higher permeation fluxes and a more efficient containment of the catalyst. The membranes are prepared by dipping a porous substrate into a solution of colloidal particles of the metal oxide or a precursor to the metal oxide (Brinker, et al., 1991). The particles are concentrated on the substrate surface through capillary action to form a gel layer (Chai et al., 1994). Adding a water-soluble compound or precursor to the sol to yield a catalyst with the desired amount of active metal forms a catalytic membrane.

Because of its value to industry, we have studied the selective hydrogenation of acetylene in a short contact time, membrane reactor. Pd supported on a γ-Al_2O_3 layer is slip cast

Correspondence concerning this article should be addressed to R. D. Gonzalez.

onto the inner surface of an α-Al_2O_3 support tube to form an annulus. The layer is well characterized and the reaction is modeled using a one-parameter dispersion equation with previously derived Langmuir–Hinshelwood expressions (Vincent and Gonzalez, 2001). The selective hydrogenation of acetylene is particularly difficult because it is a rapid, kinetically controlled reaction that may break away. We hope to determine whether the membrane can be considered as a thin film, if Knudsen diffusion is contributing and if a critical thickness exists for ethylene selectivity and conversion. We solve the nonlinear differential equation for each reactant and search for a global minimum in the error. Solutions over a 200°C temperature range should indicate the appropriateness of the reactor configuration and develop a model for its intricacies.

Experimental Methods

Preparation of γ-Al_2O_3, Pd//γ-Al_2O_3, and supported Pd membranes

For this study, two sols were created. The Pd/AlOOH sol was used as the dipping solution for the formation of a Pd/γ-Al_2O_3 catalyst membrane. The preparation of the boehmite (AlOOH) sol was based on the work of Yoldas (1975) and used as the precursor to γ-Al_2O_3. Aluminum *sec*-butoxide was mixed with excess deionized water for 15 min at 85°C, evolving butanol. The hydrolyzed product was peptized overnight at 90°C with dilute HCl in a closed container. The final molar ratios were $Al(OC_4H_9)$:H_2O:HCl equal to 1.0:100:0.07. This led to the formation of a clear, stable boehmite (AlOOH) sol. A more complete protocol is described in a previous study (Lambert and Gonzalez, 1999). Pd was introduced to the original sol by adding a designed amount of $(NH_4)_2PdCl_6$ obtained from Strem Chemicals. This precursor was added directly to the sol and stirred in a closed container for 15 min to dissolve the metal precursor. The pH of the Pd sol was measured to be 3.83.

The solution was prepared as a bath for concentrating particles on a substrate surface. The substrate, a porous α-Al_2O_3 tube, purchased from U.S. Filter under the name Membralox, was cleaned and covered with polyethylene to prevent coating of the exterior. It was then dipped into the boehmite sol for 10 s. Between each dipcoat, the tube was dried overnight at room temperature and the polyethylene film was then removed. Subsequently, the tube was calcined in an oven with a 1°C/min temperature ramp to 400°C, and maintained at 400°C for one hour. It was then cooled in a dessicator. The processes of dipping, drying, and calcining are repeated until the catalytic membrane attains a desired thickness. For some characterization studies, the remaining Pd/AlOOH sol was heated to 95°C to form a gel, and then calcined as described earlier. Two materials, an γ-Al_2O_3 and a Pd/γ-Al_2O_3 catalyst were made for characterization and reaction testing.

Membrane reactor assembly

As shown in Figure 1, the reactor body consisted of a stainless-steel outer shell through which gas could be passed. Within the outer shell was an inner shell made of stainless-steel tubing, glass, and the alumina membrane, which was connected to glass tubing with a high-temperature ceramic adhesive (Insa-Lute, #1 Paste, Sauereisen Corp., Pittsburgh, PA). The adhesive was also used to seal the ends of the tube. The glass tubing was connected to the stainless-steel tubing using Cajon (Swage-Lok) compression fittings and Kalrez O-rings.

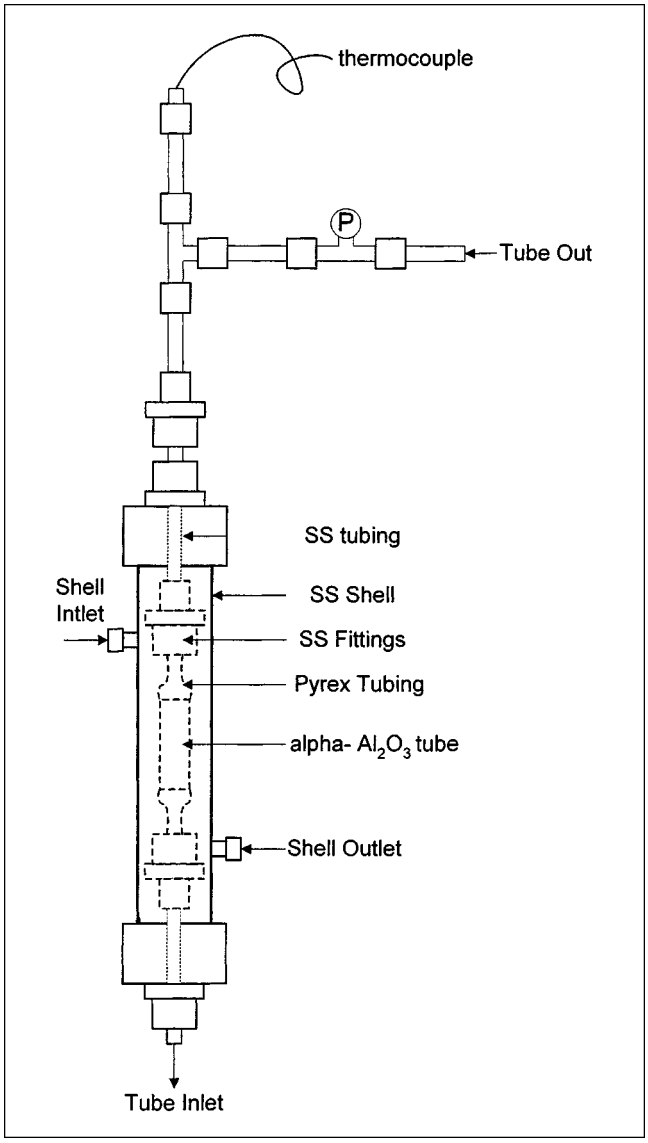

Figure 1. Testing the membrane reactor.

A K-type thermocouple extends midway down the length of the reactor and rests against the catalytic annular layer. A pressure gauge was located at the tube inlet. The outlet was plugged to create force flow radially through the membrane into the shell. The shell inlet was plugged and the outlet was allowed to vent to a fume hood. A heating tape placed on the outside of the stainless-steel shell was used to heat the reactor and the temperature was controlled using a temperature programmer.

Pretreatment and chemisorption procedure

Prior to any characterization studies, the Pd/γ-Al_2O_3 catalyst was placed in a Pyrex microreactor and heated to the pretreatment temperature of 400°C at a rate of 10°C/min. It

was calcined in flowing O_2 at 400°C for 30 min, followed by reduction in flowing H_2 at 400°C for 1 h. Flow controllers maintained a gas flow rate of 30 mL/min. A stream of Ar was used to purge the O_2 or H_2 from the reactor.

Hydrogen chemisorption was used to measure the percentage of palladium surface area in the catalyst sample. The stoichiometry of H:Pd is known to be 1:1 and the dynamic pulse method was used and has been described elsewhere (Sarkany and Gonzalez, 1982). Weakly adsorbed hydrogen, including hydrogen that may reside in bulk solution, is not measured by this method. Approximately 200 mg of pulverized catalyst was placed in a Pyrex microreactor and pretreated with a succession of gases at 30 mL/min (O_2, then Ar, and finally H_2 at 400°C). The reactor was flushed with Ar and rapidly cooled to 25°C. Small amounts of H_2 (85.8 μL) were pulsed through the reactor until saturation was achieved. A gas chromatograph equipped with a thermal conductivity detector was used to monitor the volume of H_2 exiting the reactor following each pulse. The saturation point was determined when the integrated areas from successive eluted peaks were equal. Samples were submitted to Galbraith Laboratories (Knoxville, TN) for the weight percent of Pd by the ICP method. The volume of H_2 chemisorbed was used to calculate the percentage of metal atoms with exposed surface sites.

Surface area and pore-size measurements

A Coulter Omnisorp Porosimeter was used to measure the surface area and the pore-size distribution of the membrane catalyst. A 100-mg sample was placed in a Pyrex holder, heated to 200°C, and outgassed to 10^{-5} torr. The full adsorption-desorption isotherm was obtained at 77 K using UHP nitrogen as the adsorbent. The volume of the first monolayer was calculated using the linearized BET equation. The cross-sectional area of the adsorbate molecule (0.162 nm^2) was used to estimate the surface area. The range of P/P_0 used in this calculation was 0.05 to 0.25. This is the range of the isotherm in which the monolayer is formed. The desorption branch of the isotherm is then used to generate the pore-size distribution. Pore-size distributions were also reported by U.S. Filter for the α-Al_2O_3 tube.

Scanning electron microscopy

A Cu K-α beam on a JEOL 5410 SEM at the University of New Orleans (LA) was used to observe the congruity of the catalyst membrane layer. In addition, a cross section of the catalyst membrane and substrate were examined to determine the Pd profile within the layer and possible penetration into the substrate pore system. An EDAX attachment was used in conjunction with the ZAF method for the measurement of the Pd profile concentration within the membrane layer.

Flux measurements and reaction testing

The flow system with the membrane reactor is shown in Figure 2. A bank of gases was used in this experiment: 99.999% H_2, 99.6% C_2H_2, 99.999% Ar, 99.5% pure C_2H_4, and a specialty mixture of 9.97% acetylene in Ar. They were all purchased from Tri-Gas Dousson. The H_2 and Ar were passed through a series of columns to eliminate moisture and

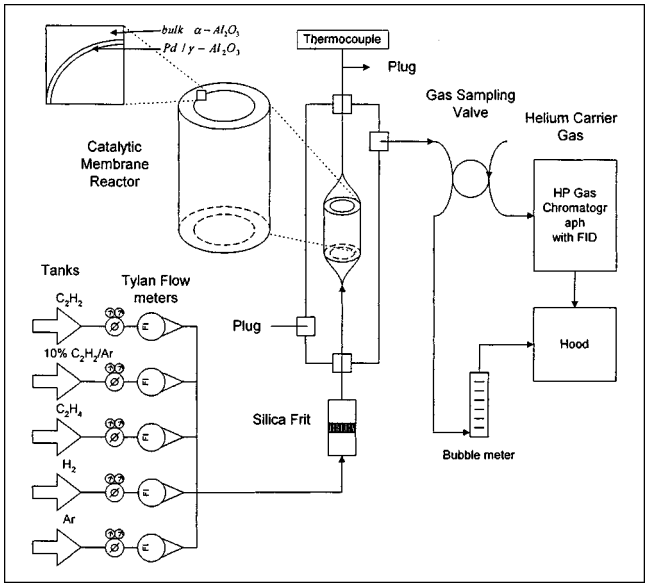

Figure 2. Membrane testing equipment.

O_2. Tylan mass flow controllers meter the exact composition and flow rate of the feed stream. They were calibrated with a bubblemeter. The gases were passed through a medium porosity silica frit (Kimble-Kontes) to assure proper mixing.

Flux measurements were made by first removing the silica frit just given. The flow rates of pure gases at different pressures and temperatures through the membrane were measured using the apparatus shown in Figure 1. The shell inlet and the tube outlet were capped in order to force the gas through the catalyst membrane and substrate wall. To calculate the flux, the gas flow rate was divided by the differential pressure across the membrane and the surface area available for flow.

The hydrogenation activity of the catalysts and supported membrane were tested using a 9.97% C_2H_2/Ar mixture as described earlier. They were reduced in H_2 for 1 h at 400°C prior to reaction in the membrane reactor. The reactions were investigated at 100, 150, 175, 200, 250 and 300°C About 200 mg of the pulverized catalysts were tested with a conventional reaction system. Each was loaded into a Pyrex microreactor and pretreated using the same standard procedure described previously for reaction (Lambert and Gonzalez, 1999). Argon was used as a diluent and pure acetylene was used to change the concentration. The total flow was approximately 28 mL/min. The mol fraction of acetylene was 7.1 mol % and the ratio of hydrogen to acetylene was 4:1. The gases then exited the shell of the steel tube into a gas-sampling valve. Pulses of the effluent were manually sampled and sent to the gas chromatograph, which was equipped with an FID detector and a Carboxen 20 column from Supelco for the separation of acetylene, ethylene, and ethane. The GC was calibrated over the range of study with dilutions of the C_2H_2 and C_2H_4 in an Ar mix. The results from the reaction tests are reported in terms of fractional conversion, X, of acetylene and molar selectivity, S, to the partially hydrogenated product, ethylene (mols of ethylene divided by total mols of product).

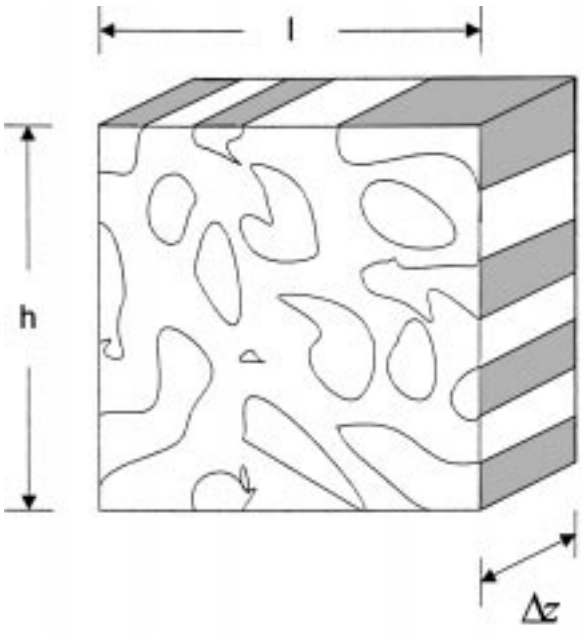

Figure 3. Mol balance on a thin film of catalyst.

Mathematical Formulation and Data Handling

In order to model successive chemical reactions through a thin catalytic layer, the one-parameter dispersion equation was chosen. Conceptually, this equation was derived by Taylor (1953) to describe laminar flow with lateral diffusion. Dankwerts (1953) adapted the model to packed beds and wrote appropriate boundary conditions. Levenspiel and Bischoff (1963) provide an excellent mathematical description, and Kreft and Zuber (1978) give a detailed explanation. Although the membrane is not a fixed bed of catalyst, we extend Taylor's model to account for either the effective Knudsen diffusion or gas dispersion in one dimension through a homogeneous medium of catalyst and modify Dankwerts' boundary conditions. Changes in volume and geometric effects are omitted. Shown in Eq. 1 is the mass flux balance for species i through a differential thickness, Δz, of catalyst, which is shown in Figure 3

$$D_i \frac{d^2C_i}{dz^2} - \frac{duC_i}{dz} + \frac{\rho_c r_i'}{\epsilon} = 0 \tag{1}$$

where C_i is the concentration of species, i, within the porous structure, and u is the interstitial velocity. The rate of reaction is designated by r_i', the density is ρ_c, and ϵ is the void fraction, while D_i may represent either the effective Knudsen diffusion or gas-dispersion. The effective Knudsen diffusion will be referred to simply as Knudsen diffusion in the remainder of the text. It is often present in the pores of catalysts and may contribute to the model. For packed beds, dispersion often represents the separation of streamlines as perturbation occurs upon entrance into the catalyst bed (Kreft and Zuber, 1978). Gas dispersion is a general indication of the level of back mixing into the system. By nondimensionalizing, Eq. 2 is obtained. The mol fraction under constant molar flow conditions (P and T may vary) is y_i, and z is replaced by λ for a thickness, t

$$\frac{D_i}{ut}\frac{d^2y_i}{d\lambda^2} - \frac{dy_i}{d\lambda} + \frac{RT}{P}\frac{\rho_c t r_i'}{u\epsilon} = 0 \tag{2}$$

For successive reactions, the rate expression for Eq. 2 may be quite complex. It might contain multiple mechanisms for both consumption and generation. To simplify this idea, Eq. 3 is introduced. Each mechanism is denoted by variable j

$$r_i' = \sum_{j=1} \nu_i k_{ij} f_{ij}(y) P^2 \tag{3}$$

Each term in equation 3 has a rate constant that yields another unknown. If the internal ratio of the rate constants is known, then a reduced form may be rewritten in Eq. 4.

$$\frac{r_i'}{k_{i1}P^2} = f_{i1}(y) + \sum_{j=2} \nu_i \kappa_{ij} f_{ij}(y) \tag{4}$$

where κ_{ij} is the ratio of the rate constants, and the total mass balance can now be expressed in terms of two dimensionless quantities, the Peclet and Damköhler numbers (Pe_i and Da_i) respectively (see Eq. 5)

$$\frac{1}{Pe_i}\frac{d^2y_i}{d\lambda^2} - \frac{dy_i}{d\lambda} + Da_i\left(f_{i1}(y) + \sum_{j=2} \nu_i \kappa_{ij} f_{ij}(y)\right) = 0 \tag{5}$$

This equation is written with respect to $f_{i1}(y)$, the primary mechanism. The Peclet number is the ratio of bulk flow to either diffusive or gas-dispersed flow, and the Damköhler number is the ratio of the rate of the primary reaction path to bulk flow, while P^2 results by assuming that a surface reaction between two adsorbed species occurs. For the successive reactions, i may represent C_2H_2, C_2H_4, C_2H_6, or H_2. With two reactions, this yields four equations with a total of six unknowns (4 Pe_i and 2 Da_i).

P.N. Dankwerts (1953) originally derived the boundary conditions necessary for solution. He was able to show that for a closed-closed system, a flux balance at the entrance and exit of the catalyst bed were necessary in order to solve the differential equations. With gas-dispersion, closed-closed signifies that no concentration distribution exists at the entrance or exit. Thus, the change in concentration is not a statistical quantity. A total mass balance at the entrance accounts for viscous flow, diffusion (or dispersion), and reaction. A general derivation of the boundary conditions at the entrance and exit is shown in Figure 4. Flow enters via viscous transport only; y_{i0} is the entering concentration. Viscous flow and dispersion exit the boundary. Reaction at the surface is possible, and we assume that the area available for reaction is $(1-\epsilon)$. Thus, the boundary condition is modified in Eq. 6. It is made dimensionless and we assume that no pressure or temperature change occurs across the boundary

$$y_{i0} = y_i|_{\lambda\to 0^+} - \frac{1}{Pe_i}\frac{dy_i}{d\lambda}\bigg|_{\lambda\to 0^+} + Da_i\,\chi\left(f_{i1}(y) + \sum_{j=2} \nu_i \kappa_{ij} f_{ij}(y)\right) = 0 \tag{6}$$

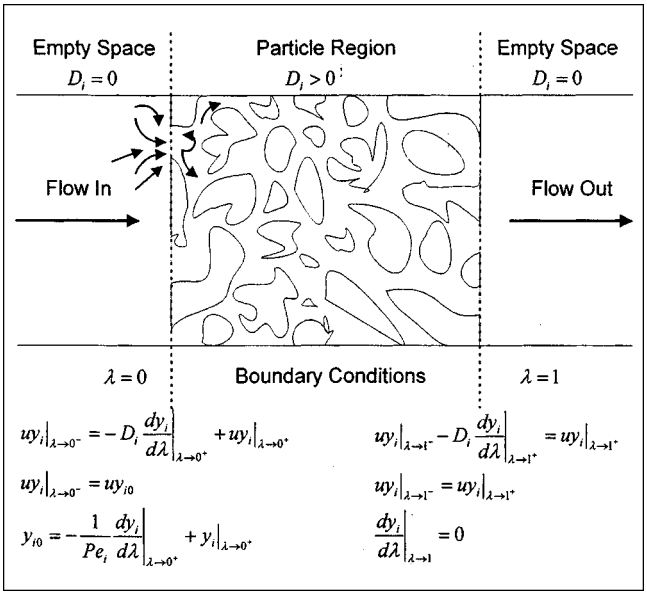

Figure 4. General derivation of the boundary conditions.

Importantly, χ is the ratio of external surface area to the BET surface area, S_A (Eq. 7)

$$\chi = \frac{(1-\epsilon)}{\rho_c S_a t} \tag{7}$$

At the exit, the classic derivation considers that the concentration entering and exiting the boundary are equal. Thus, the concentration gradient of species i without volume, pressure, or temperature change must be zero

$$\left.\frac{dy_i}{d\lambda}\right|_{\lambda\to 1} = 0 \tag{8}$$

Kinetics

In order to solve Eq. 5 with the boundary conditions in Eqs. 7 and 8, the kinetics of both acetylene consumption and ethane formation must be known. As expressed previously, the actual mechanistic steps derived for acetylene reaction on the surface of the catalyst are quite complex. Two recent reviews by Bond (1997) and Bos et al. (1993) are explanatory. Although the number of proposed Langmuir–Hinshelwood mechanisms is vast, several recent efforts by Borodzinski and Cybulski (2000) and Vincent and Gonzalez (2001) have combined both spectroscopic evidence, and the many results of previous studies to present Eqs. 9 and 10 for acetylene consumption and ethane formation, respectively. These studies were performed in a differential reactor. However, it is crucial to this work to concisely summarize their development and exclusions in order to understand their limitations

$$-r'_{Ac} = \frac{k_{Ac1} y_{Ac} y_{H_2} P^2}{(1+K_{Ac} y_{Ac} P)^2} + \frac{k_{Ac2} y_{Ac} y_{H_2} P^2}{(1+K_{Ac} y_{Ac} P)\left(1+K_2\sqrt{y_{H_2} P}\right)} \tag{9}$$

$$r'_{Ea} = \frac{k_{Ea1} y_{Et} y_{H_2}^{1/2} P^{3/2}}{(1+K_{Ac} y_{Ac} P)} + \frac{k_{Ea2} y_{Et} y_{H_2} P^2}{(1+K_{Ac} y_{Ac} P)\left(1+K_2\sqrt{y_{H_2} P}\right)} \tag{10}$$

The first terms in Eqs. 9 and 10 will be designated as primary for this study. Vincent and Gonzalez (2001) derived them specifically for the temperature range of this study. They can be made to fit the form of Eq. 4. Rate data were analyzed for reactant dependencies and activation energies. A Levenberg–Marquardt algorithm was then applied to the integral reactor design equation to discriminate among rival mechanisms, and the temperature-dependent values were regressed. The work of Borodzinski and Cybulski (2000) derived a four-term equation for the hydrogenation of acetylene over supported Pd and solved for its parameters at 25°C. One path involves the formation of C4s, one directly to ethane and two to ethylene. Beebe and Yates (1986) were able to show that on Pd the direct formation of ethane from acetylene through ethylidine is very small, and Borodzinski and Cybulski (2000) also showed that the formation of C4s is small with dilute reactants. The two terms of Eq. 9 represent the formation of ethylene via two parallel paths. The first term involves the competitive adsorption of acetylene on the Pd surface. The second term involves the noncompetitive adsorption of atomic hydrogen and acetylene, in which hydrogen is transferred from a carbonaceous deposit (Bos et al., 1993) on the Pd surface. Importantly, as temperature increases, Vincent and Gonzalez (unpublished results, 2001) were able to show that the second term becomes dominant and passes through a maximum. For ethane formation, nearly identical mechanisms exist, except that the first addition of hydrogen was found to be rate determining in the first term. The carbonaceous deposit path (second term) was found to only make a minor contribution to the total rate of ethane formation.

Results

Physical properties of catalysts and membrane materials

The α-Al_2O_3 substrate was prepared according to the procedure just described, and the cumulative weight gains are shown in Figure 5. After the initial dip, the incremental gains in weight are much smaller. The total weight of the catalyst membrane is 0.0255 g. The general physical properties, such as surface area, pore-size, and percent metal exposed, are shown in Table 1 for the membrane catalyst and for comparison to the Pd/γ-Al_2O_3 catalyst used for previous kinetic studies (Vincent and Gonzalez, 2001). The blank γ-Al_2O_3 had structural properties, which were similar to those of the membrane. They were prepared by nearly identical methods. All three have very similar properties and show a similar pore-size distribution (Figure 6). Although the metal loading for the kinetic study was lower (to reduce conversion), the results were applicable to our membrane studies.

The radial profile of Pd loading within the catalyst and extending into the substrate is shown in Figure 7. The Pd concentrations do vary, but correspond very well with the ICP analysis (by Galbraith). A sharp decline in Pd concentration is observed between the points along the interface and suggests that capillary action was not strong enough to draw Pd

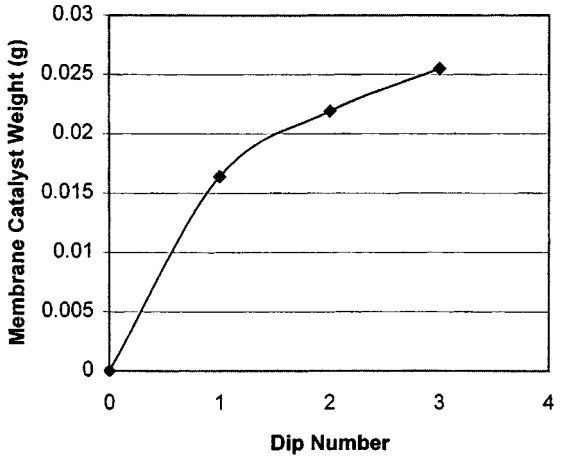

Figure 5. Membrane thickness vs. number of dipcoats.

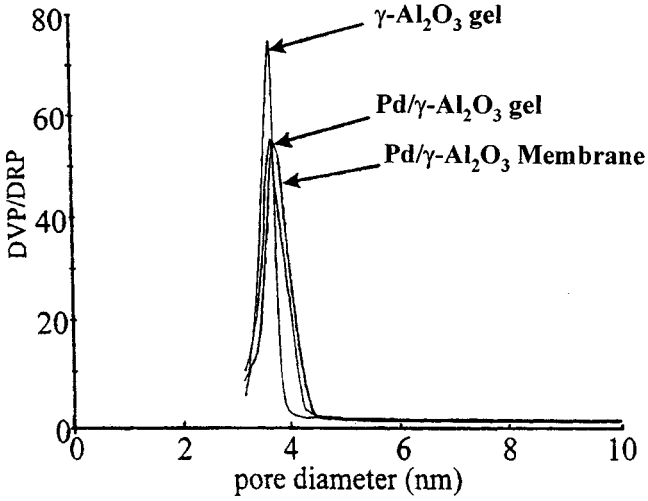

Figure 6. Comparison of the gel catalyst for kinetic study and the membrane.

Unimodal pore-size distributions exist for γ-Al_2O_3 gel, Pd/γ-Al_2O_3 gel, and the Pd/γ-Al_2O_3 membrane (from BET desorption isotherm).

into the substrate. This reasonably indicates that the active metal for this reaction, Pd, is within the catalyst layered on the surface of the tube support. The observed surface has no obvious cracks or fissures (confirmed by multiple pictures to SEM resolution), and the catalytic layer is only about 5 μm thick and corresponds well to an average thickness of 8.4 μm. As shown in Figure 8, the α-Al_2O_3 tube has three pore-size sections and only the smallest (200 nm) is mesoporous.

For the mathematical model, Figure 7 is in accord with our assumption of a thin film, and the high BET surface area yields a value of 7.4×10^{-5} for χ in the entrance boundary condition. Thus, its term is truncated from Eq. 6. Correspondingly, less area is exposed at the exit from the buttress of the substrate (Figure 7), and reaction at this boundary is also neglected. As the reactant mixture exits the catalyst and enters the substrate, the pore-size structure increases, reducing constriction to flow. The traditional Dankwert's boundary condition is therefore sufficient.

Acetylene hydrogenation

In Figure 9, the experimental result of selectively hydrogenating acetylene with excess hydrogen is shown. Two runs vs. temperature were performed to duplicate the trend seen in the data. A maximum in conversion is observed at approximately 200°C. The selectivity is observed to increase with temperature. Notably, a break in selectivity is observed at 175°C. Importantly, hydrogen was fed in excess of the stoichiometric ratio to delineate that the observed selectivity occurs independent of a limiting reagent. In addition, excess hydrogen is known to retard rapid coke formation (Albers et al., 1999), which leads to catalyst deactivation. The low acetylene content is similar to industrial feeds. Excess ethylene is not included because a natural increase in selectivity will occur with decreased space time. Under the conditions of this study, the concentration of acetylene is dilute and data were taken after 6 h, so that C4 formation was small and at steady state. C4 is then excluded from the mol balance. Pure γ-Al_2O_3

Table 1. Catalyst and Membrane Characteristics

Characteristics	Memb. Catal.	Catalyst for Kinetics ‡
Pd (wt. %)	1.3	0.2 %
Density	2.3	2.8 g/cm^3
Memb. thickness or particle dia.	8.4	5.0 μm
BET area	334	366 m^2/g
Avg. pore dia.*	3.6	3.6 nm
Pore volume	0.37	0.31 cm^3/g
Surface metal exposed, *Sm* (%)**	29	32 %
Avg. Pd particle dia.†	3.4	3.1 nm

*From BET desorption isotherm.
**Dispersion as measured by hydrogen chemisorption, H:Pd surface = 1:1.
†Metal particle diameter ($98.2/S_m$), assuming Pd density = 11.40 g/cm^3.
‡Vincent and Gonzalez (2001).

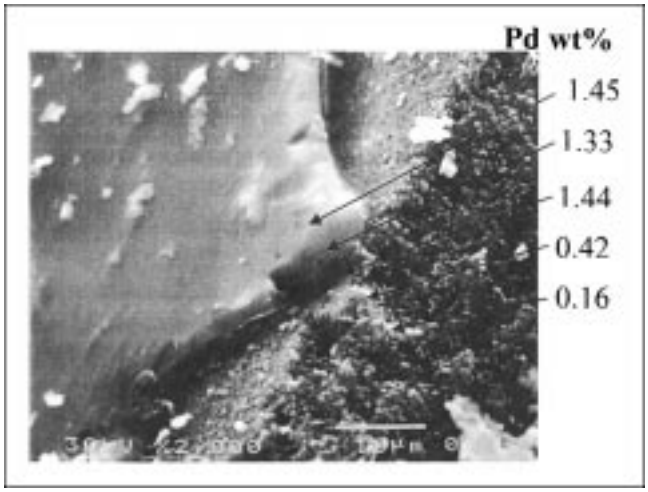

Figure 7. SEM with EDX overlay: Pd concentration along the radius of annular catalytic layer and into support tube.

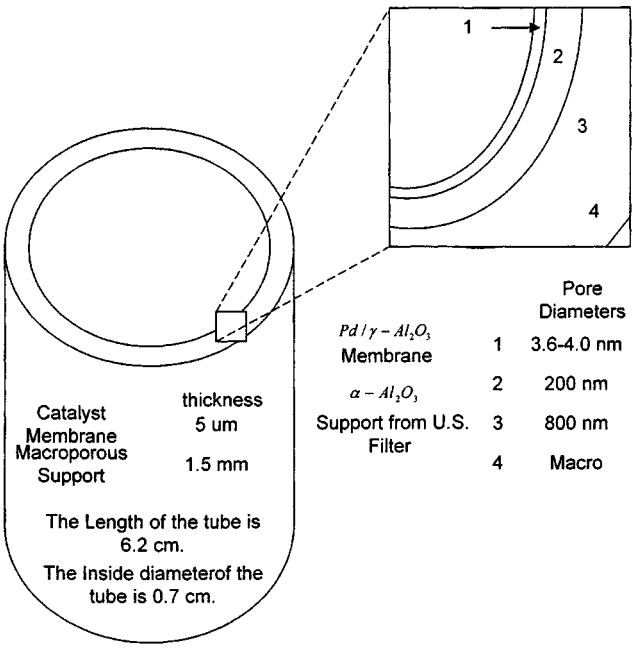

Figure 8. Pore diameter for the membrane and α-Al_2O_3 tube.

showed no reactivity and an equal weight of pulverized Pd/γ-Al_2O_3 catalyst showed no selectivity in a packed-bed reactor.

Flux experiments

Figure 10a and 10b show the experimental flux rate dependencies on gas species and temperature, respectively. Only the data obtained at 25°C are shown in Figure 10a. The permeability is measured as a function of pressure drop across the membrane and a limiting value is reached with increasing pressure. With the exception of hydrogen, the ratio of the values corresponds well to the ratio of the inverse of the square-root ratio of their molecular weights. The permeability of hydrogen was one half that expected. This is seemingly consistent with a Knudsen mechanism and did not vary with temperature. Figure 10b shows the permeability as a function of temperature at constant absolute pressure (202.7 kPa). The trend does not correlate to a negative square-root dependence in temperature, but rather decreases exponentially. This contends that gas dispersion and not Knudsen diffusion is dominant.

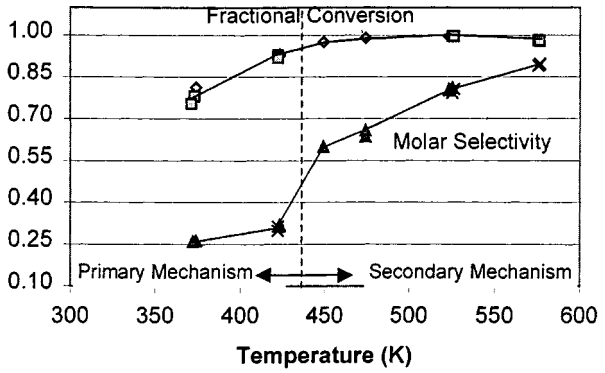

Figure 9. Conversion (Run 1 ■, Run 2 ♦), and selectivity (Run 1 × and Run 2 ▲) in a Pd/γ-Al_2O_3 catalytic membrane reactor.

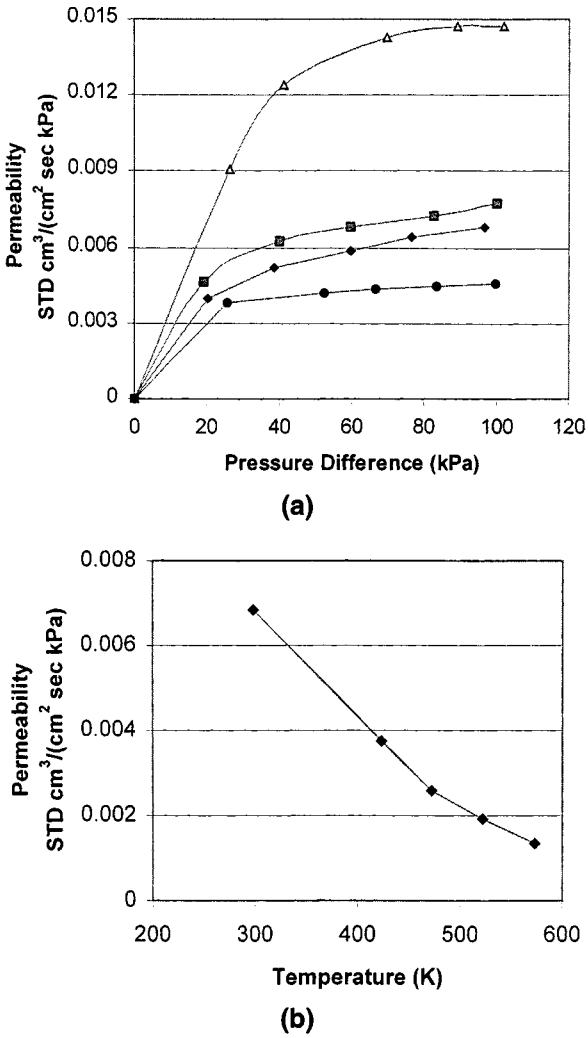

Figure 10. Permeability study: (a) C_2H_2 ■, C_2H_4 ♦, Ar ●, and H_2 ▲ at 25°C; (b) C_2H_2 vs. temperature at 202.7 kPa.

The dispersion model

The Peclet numbers should be inversely proportional to the measured gas dispersion. Acetylene, hydrogen, ethylene, and ethane are in dilute concentrations in the feedstream and should have approximately the same dispersion ($Pe_i = Pe_{Ar}$). This was justified based upon Wilke's equation (1950) for mixed diffusion. Importantly, two components would have to be appreciably concentrated to change this result (only Ar is). The numerical differential equation solver in Mathematica 4.0 is then used to solve the DEQs for all the reactive components. An iterative technique is used that requires knowledge of two boundary conditions at one of the boundaries. Dank-

wert's exit condition and the exit concentrations are known. The entrance boundary condition was rewritten as an error function for each species (Eq. 11). Importantly, no entrance gas dispersion exists for ethylene or ethane

$$\text{error}_i = \frac{\left| y_i|_{\lambda \to 0^+} - \frac{1}{Pe_i} \frac{dy_i}{d\lambda}\Big|_{\lambda \to 0^+} - y_0 \right|}{y_{i,\text{average}}} \tag{11}$$

Their errors are based then on initial concentration (zero).

The Peclet numbers for each gas are related to ethylene and the differential equations are then solved for a variety of Pe_{Ac} and Da_{Ac} (at constant Da_{Ea}/Da_{Ac}) pairs for each set of conversion and selectivity data shown in Figure 9 to produce a locus of minima in error. In Figure 11a, the locus of minima for hydrogen at 150°C is shown. The curve shows the dependence of the Peclet number on the Damköhler number for a solution. A total solution will require the convergence of the solutions to three DEQs (three unknowns) to a single value. As there are four equations and only three are necessary for convergence, there are four possible solutions. With the data's error, some difference may exist between the solutions. Thus, a solution is found by minimizing the square root

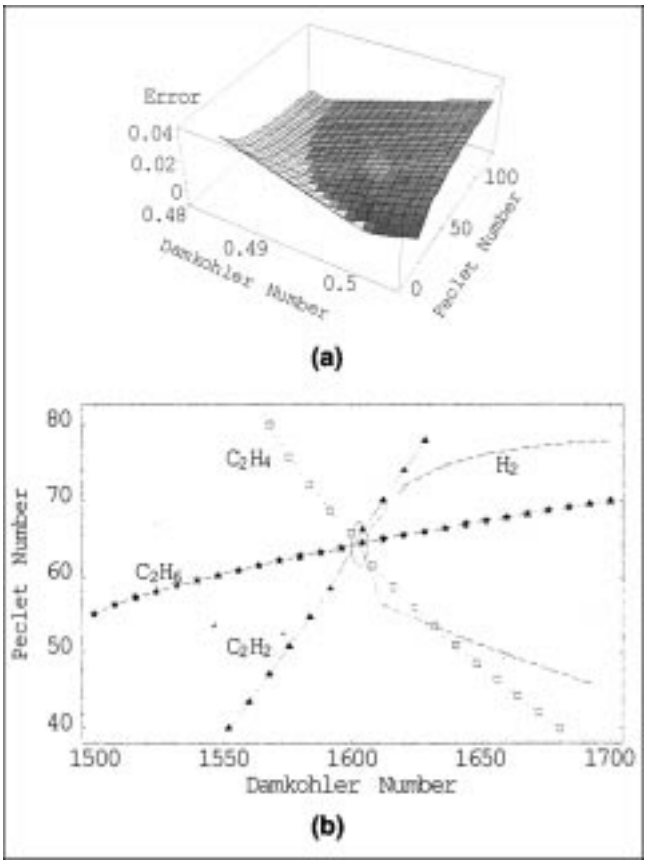

Figure 11. (a) Locus of minima for the solution to H_2 differential equation at 150°C; (b) its convergence for C_2H_2 ▲, C_2H_4 □, C_2H_6 ★, and H_2 × at 100°C.

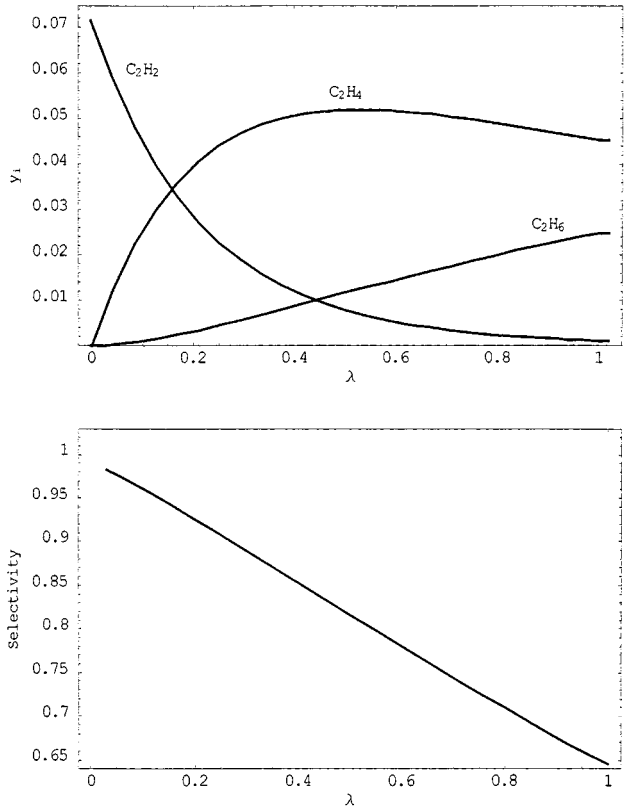

Figure 12. Model solution at 200°C through membrane thickness: (a) concentration; (b) selectivity.

of the sum of the errors. As shown in Figure 11b, the four DEQs converge to nearly the same value (Pe_{Ac}, Da_{Ac}, $Da_{Ea}/Da_{Ac} = 64.24$, 1604.5, 0.0701) for 100°C and represent the minima in total error (1.3%, which is much better than the experimental error of 4%). An example of the concentration distribution and selectivity are shown in Figure 12a and 12b, respectively. Figure 12a shows how acetylene is consumed, ethylene reaches a maximum, and ethane is produced at 200°C as a function of dimensionless thickness. The ethylene maximum corresponds to the critical thickness within the bed. It represents a contact time of 8.2×10^{-3} s (residence time * void fraction). Figure 12b delineates that the highest selectivity is at the entrance, when no ethylene or ethane is present initially. The example results presented are representative of the other temperatures.

Comparatively, the Peclet number solutions and Damköhler number solutions match the expected trends and values for dispersion and rate constant, respectively, as a function of temperature. In Figure 13a, the Peclet number is plotted on the left *y*-axis and the inverse gas-dispersions from the flux data on the right *y*-axis. They differ only by a constant, as expected. The rate constants for each temperature for the primary mechanism of acetylene are transformed back to the percent metal exposed and metal loading of the catalyst used for kinetics (Vincent and Gonzalez, 2001) and show good correlation in Figure 13b. A void fraction of 0.5 was

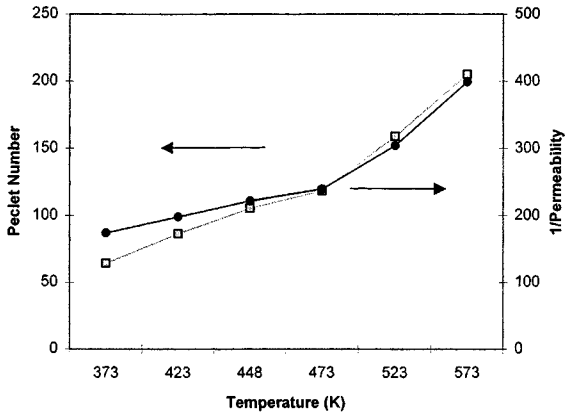

(a)

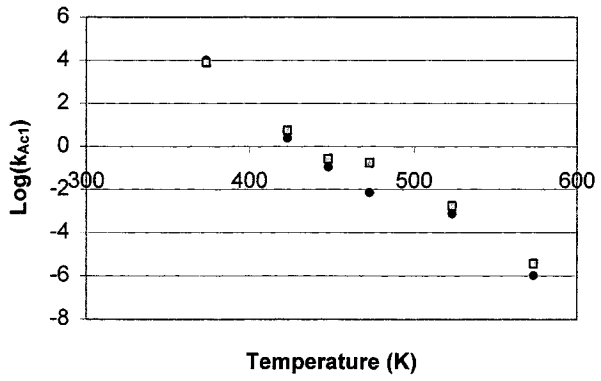

(b)

Figure 13. (a) Peclet number solution vs. permeability results vs. temperature; (b) primary rate constant for acetylene as calculated from Damköhler number ■ and predicted by the kinetics (Vincent and Gonzalez, unpublished results, 2001) ●.

assumed. The log plot shows only a slight deviation at 175°C. With good correlation of the rate constants, the average residence time is calculated from the Damköhler number to be 0.019 s. This corresponds very well to an estimated value of 0.015 s (from ρ_c and volumetric flow rate).

As a function of temperature, the critical thickness increases (Figure 14a). We explain this result with the kinetics. The ratio of the effective rate constants in Figure 14b shows that only at 100°C is the rate of ethane formation favored kinetically. The effective rate constant is calculated by $k_{eff,Ea}/k_{eff,Ac} = (r'_{Ea}\ y_{Ac,0})/(-r'_{Ac}\ y_{Et,0})$. The ratio decreases with temperature and the selectivity increases, needing more catalyst to achieve its maximum (thus a longer residence time). It is important to note that the rates of reaction of acetylene and ethylene increase with thickness at 100°C, but decrease at 150°C (Figure 15). This change also corresponds to the change of the ratio of effective rate constants in Figure 14b. Acetylene poisons both reactions, so that both reactions increase at 100°C with its consumption. However, the adsorption of acetylene is no longer important at 150°C (Vincent and Gonzalez, unpublished results, 2001), and the rates decrease with consumption of their respective reactants.

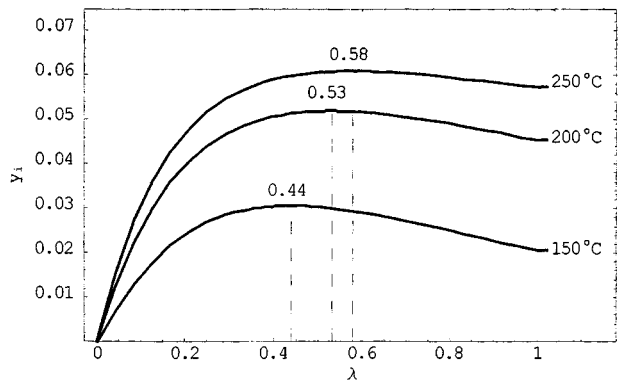

(a)

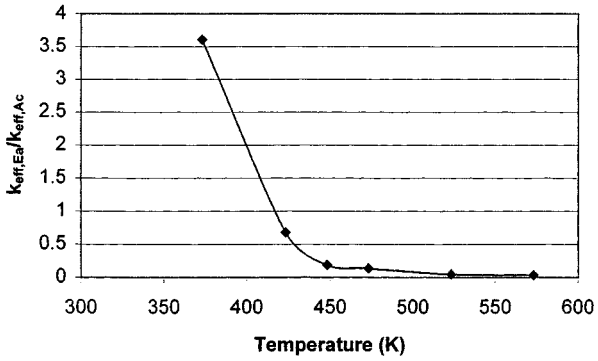

(b)

Figure 14. (a) Critical thickness vs. temperature; (b) ratio of the effective rate constant for C_2H_2 to C_2H_6.

Discussion

Membrane reactors have many applications in heterogeneous catalysis. Coronas and Santamaría (1999) provide a good overview of reviews, configurations, materials of construction, and appropriate applications. Some applications promote equilibrium shift reactions by product removal, coupling of oxidation, and reduction reactions on the opposite

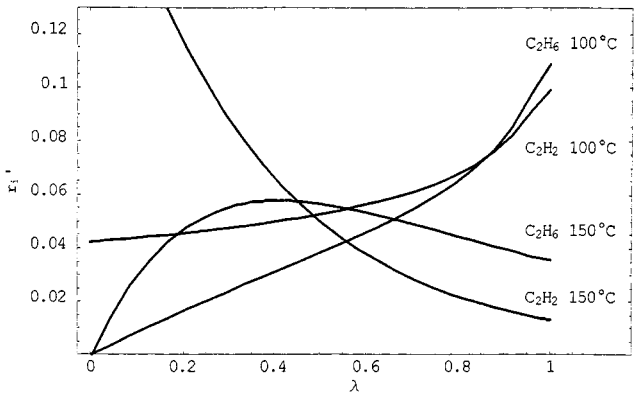

Figure 15. Comparison of reaction rates from the model solution for C_2H_2 consumption and C_2H_6 production at 100 and 150°C

sides of the membrane and maximize conversion and selectivity of intermediate compounds. The latter is the subject of this discussion and was considered theoretically by Berstein and Lund (1993). They found an application in which the rate constant for the successive reaction is an order of magnitude faster than the first reaction. In this study, we investigated the use of a thin catalytic layer as a short contact time reactor with a dispersion model with complex kinetics. Particularly, acetylene inhibits both reactions and multiple mechanisms contribute to their rates. Other reactor configurations with different geometry, such as the monolith or gauze, are also possible, but they do not force contact of the feedstream with the catalyst (and thus eliminate external mass transfer). Our configuration eliminates catalyst bypass.

Initially, we had concerns of possible mass-transfer limitations interfering with our kinetic expressions. In the SEM study of the catalyst, the surface appears devoid of cracks and fissures. The dip-coat method was observed to correct minor flaws by filling and creating a contiguous catalytic layer, which has not infiltrated the substrate. With the highest of conversions occurring at the highest kinetic rates, any mass-transfer gradients are probably small. The high Peclet number also indicates that the force flow situation eliminates any external mass-transfer limitation as the gas is forced to contact the catalyst. We showed that internal mass-transfer limitations do not exist in the powdered catalyst (Vincent and Gonzalez, unpublished results, 2001). Thus, with a particle diameter comparable to the thickness of the membrane, the kinetics correlated well to the previous study, and mass-transfer limitations are absent.

The dispersion model accurately described flow within the thin catalyst layer and was similarly applied in several studies with the exception of Sloot et al. (1992), who used the dusty gas model. We also neglected the change in volume with reaction as studied by Sun and Khang (1990), because of sufficiently dilute concentrations. In addition, the effect of axial dispersion within the void space of the tube was neglected. Koukou et al. (1996) used a full set of partial differential equations to describe the dehydrogenation of cyclohexane in a catalytic ceramic annulus. From their results, a very high tube length to tube inner diameter ratio would be necessary to affect gas dispersion within our membrane. Lastly, Koukou et al. (2001) included the implications of heat transfer and enthalpy of reaction on nonideal effects in membrane reactors.

Industrially, this reaction is performed at much higher pressures and lower temperatures. However, the kinetics could probably not be extrapolated to these conditions, but valuable insight into the performance of this reactor was obtained. Although permeability data vs. temperature suggested an effective Knudsen diffusion (a ratio of the square root of the molecular weights), neither permeability vs. temperature data nor modeling results concur. An effective Knudsen diffusion would also have a square-root dependence upon the temperature and a minus square-root dependence for the Peclet number. Figure 13a shows the inverse permeability and Peclet number actually increased with temperature (nearly exponential) rather than decrease as expected. In addition, a Peclet number corresponding to an effective Knudsen diffusion must be less than approximately 2. The lowest Peclet number calculated was about 64 (at 100°C). This is then attributed to gas dispersion, which must provide a greater resistance to flow. The magnitude and behavior of the Peclet number with temperature indicated that flow dispersion changes from intermediate to small with inceasing temperature (Levenspiel and Bischoff, 1963). Lange et al. (1998) provided the most comparable study, in which the selective hydrogenation of 2-hexyne to *cis*-2-hexene occurs on a ceramic-supported sol–gel-prepared Pt catalyst. Although the reaction is controlled by the permeation of hydrogen through the membrane, the unusual selectivity results from the reduction of hydrogen flux from pore blocking via carbon deposits. In contrast, our high selectivity results from a short contact time similar to the ultrathin membranes (Gryanznov et al., 1981; Itoh et al., 1993).

For the $Pd/\gamma\text{-}Al_2O_3$ membrane, acetylene inhibits both reactions at low temperatures. However, ethylene hydrogenation will accelerate, once acetylene reaches very low concentrations. This is very difficult to control. It might be easier to control the selectivity and conversion of this reaction with a catalytic membrane at a slightly higher temperature where the kinetics are more favorable. Although the selectivity increases with temperature, coking on the catalyst also increases (Larsson et al., 1998). Thus, a midpoint must be found to provide high selectivity with longevity.

Our dilute concentrations model the industrial feed in which the bulk constituent is ethylene. In both cases the highest selectivity will always occur at the entrance when the rate of acetylene hydrogenation is greater than ethylene. With short contact times, the kinetics will always control the selectivity and critical thickness for maximizing concentration. Selectivity will continue to decrease as ethylene is consumed and ethylene concentration is maximized when residence times are low. Unless a method for converting ethane to ethylene exists, some ethylene will always be consumed. In practice, the short contact times (and higher selectivity) may be extended for industrial feeds by applying a bank of supported membrane tubes similar to a heat exchanger. The dip-coat method enables tailoring of the thickness. Combined with the length of the tube, they control the residence time and selectivity. Better catalysts that increase the selectivity at the critical thickness will always facilitate this approach to higher conversions and control.

Conclusions

Industrially, high conversion coupled with high selectivity is desired. The short-contact-time reactor will not exceed the natural selectivity of the catalyst, but may allow conversion to the intermediate product to be maximized with some reduced selectivity in fast reactions. Selectivity will increase by decreasing the contact time, but the conversion will decline to zero after passing through the maximum. The maximum occurs at the critical thickness, which is determined by the kinetics in this reactor. With the appropriate preparation of the sol, dip-coats will result in thinner layers without defects and achieve the critical thickness. Transport is affected by gas-dispersion and not Knudsen diffusion.

Lastly, ceramic membranes offer several advantages over thin metal membrane in short contact time reactors: high permeability, thermal stability, low-pressure drop, and efficient containment of the catalyst. From this study, two addi-

tional benefits are assigned: tailoring of residence times and applying more complex catalysts for specific reactions. For example, our catalyst has a very narrow pore-size distribution, which would be impossible to obtain with a pure metal. In conclusion, we demonstrate that ceramic membranes with low metal loadings may facilitate conversion and selectivity in short-contact-time reactions when ultrathin metal membranes would be too thin to offer practicality.

Acknowledgments

The authors acknowledge support from the U.S. Department of Energy, Basic Energy Sciences (DOEFG02-86ER-1351), the Louisiana Board of Regents in the form of a BOR Fellowship to Mathew J. Vincent, and the National Science Foundation.

Notation

$A = hl$
C_i = concentration of specie i, mol/L
$Da_i = (\rho_c k_{ij} tPRT)/(u\epsilon)$
Di = gas dispersion or diffusion of species, i, m^2/s
h = height of layer, m
i = species of acetylene, ethylene, ethane, hydrogen, or argon
j = counter for multiple mechanisms
K_{Ac} = equilibrium constant for acetylene adsorption, kPa^{-1}
K_2 = equilibrium constant for hydrogen transfer mechanism, kPa^{-1}
k_{ij} = biomolecular rate constant for species i, mechanism j, $mol/(g_{cat} \cdot s \cdot atm^2)$
l = width of layer, m
n_i = mols of species i, mol
P = pressure, kPa
$Pe_i = (ut)/D_I$
R = ideal gas constant, (L·atm)/(mol·K)
r_i' = rate of reaction of species, i, mol reacted per weight catalyst $mol/(g_{cat} \cdot s)$
$S = n_{Et}/(n_{Et} + n_{Ea})$
S_A = BET surface area, m^2/g
S_m = surface metal exposed, %
T = temperature, K
t = thichness of the catalytic membrane, m
u = interstitial velocity, m/s
$X = 1 - n_{Ac}/n_{Ac,0}$
y_i = mol fraction of species i, (i mols/total mols)
z = length direction, m

Greek letters

$\chi = (1 - \epsilon)/(\rho_c S_A t)$, ratio of inner surface area to bulk surface area
ϵ = catalyst void fraction
$\kappa_{ij} = k_{ij}/k_{il}$, internal ratio of rate constants for specie i to the primary mechanism
$\lambda = z/t$
ν_i = stoichiometric coefficient for species, i
ρ_c = catalyst density, g/cm^3

Literature Cited

Albers, P., K. Seibold, G. Prescher, and H. Muller, "XPS and SIMS Studies of Carbon Deposits on Pt/Al_2O_3 and Pd/SiO_2 Catalysts Applied in the Synthesis of Hydrogen Cyanide and the Selective Hydrogenation of Acetylene," *Appl. Catal. A*, **176**, 135 (1999).

Armor, J. N., "Membrane Catalysis: Where Is It Now, What Needs to Be Done?" *Catal. Today*, **25**, 199 (1989).

Beebe, T. P., Jr., and J. T. Yates, Jr., "An in Situ Infrared Spectroscopic Investigation of the Role of Ethylidyne in the Ethylene Hydrogenation Reaction on Pd/Al_2O_3," *J. Amer. Chem. Soc.*, **108**, 663 (1986).

Benner, L. S., T. Suzuki, K. Meguro and S. Tanaka, *Precious Metals: Science and Technology*, The International Precious Metals Institute, Allentown, PA (1991).

Berstein, L. A., and C. R. F. Lund, "Membrane Reactors for Catalytic Series and Series-Parallel Reactions," *J. Membr. Sci.*, **77**, 155 (1993).

Bond, G. C., *Catalysis by Metals*, Academic Press, New York (1962).

Bond, G. C., "The Role of Carbon Deposits in Metal-Catalysed Reactions of Hydrocarbons," *Appl. Catal. A*, **149**, 3 (1997).

Borodzinski, A., and A. Cybulski, "A Kinetic Model of Hydrogenation of Acetylene–Ethylene Mixtures Over a Palladium Surface Covered by Carbonaceous Deposits," *Appl. Catal. A*, **198**, 51 (2000).

Bos, A. N. R., and K. R. Westerterp, "Mechanism and Kinetics of the Selective Hydrogenation of Ethyne and Ethene. A Review," *Chem. Eng. Processes*, **32**, 1 (1992).

Bos, A. N. R., F. Foeth, E. Bootsma, H. Sleyster, and K. Westerterp, "A Kinetic Study of the Selective Hydrogenation of Ethyne and Ethene on a Commercial Pd/Al_2O_3 Catalyst," *Chem. Eng. Processes*, **32**, 53 (1993).

Brinker, C. J., G. C. Frye, A. J. Hurd, and C. S. Ashley, "Fundamentals of Sol-Gel Dip Coating," *Thin Solid Films*, **201**, 97 (1991).

Chai, M., M. Machida, K. Eguchi, and H. Arai, "Preparation and Characterization of Sol-Gel Derived Microporous Membranes with High Thermal Stability," *J. Membr. Sci.*, **96**, 205 (1994).

Coronos, J., and J. Santamaría, "Catalytic Reactors Bases on Porous Ceramic Membranes," *Catal. Today*, **51**, 377 (1999).

Dankwerts, P. N., "Continuous Flow Systems. Distribution of Residence Times," *Chem. Eng. Sci.*, **2**, 1 (1953).

Gates, B. C., J. R. Katzer, and G. C. A. Schuit, *Chemistry of Catalytic Processes*, McGraw-Hill, New York (1979).

Gryaznov, V. M., V. Smirnov, and M. G. Slin'ko, "The Development of Catalysis by Hydrogen Porous Membranes," *Stud. Surf. Sci. Catal.*, **7**, 224 (1981).

Itoh, N., W. C. Xu, and A. M. Sather, "Capability of Permeate Hydrogen through Palladium-Based Membranes for Acetylene Hydrogenation," *Ind. Eng. Chem. Res.*, **32**, 2614 (1993).

Koukou, M. K., N. Papayannakos, and N. C. Markatos, "Dispersion Effects on Membrane Reactor Performance," *AIChE J.*, **42**, 2607 (1996).

Koukou, M. K., N. Papayannakos, and N. C. Markatos, "On the Importance of Non-Ideal Flow Effects in the Operation on Industrial-Scale Adiabatic Membrane Reactors," *AIChE J.*, **83**, 95 (2001).

Kreft, A., and A. Zuber, "On the Physical Meaning of the Dispersion Equation and Its Solutions for Different Initial and Boundary Conditions," *Chem. Eng. Sci.*, **33**, 1471 (1978).

Lam, W. K., and L. Lloyd, "Catalyst Aids Selective Hydrogenation of Acetylene," *Oil Gas J.*, **70**, 66 (1972).

Lambert, C. K., and R. D. Gonzalez, "Activity and Selectivity of a $Pd/\gamma\text{-}Al_2O_3$ Catalytic Membrane in the Partial Hydrogenation Reactions of Acetylene and 1,3-Butadiene," *Catal. Lett.*, **57**, 1 (1999).

Lange, C., S. Storck, B. Tesche, and W. F. Maier, "Selective Hydrogenation Reactions with a Microporous Membrane Catalyst, Prepared by Sol–Gel Dip Coating," *J. Catal.*, **175**, 280 (1998).

Larsson, M., J. Jansson, and S. Asplund, "The Role Coke in Acetylene Hydrogenation on $Pd/\gamma\text{-}Al_2O_3$," *J. Catal.*, **178**, 49 (1998).

Levenspiel, O., and K. B. Bischoff, "Patterns of Flow in Chemical Process Vessels," *Adv. Chem. Eng.*, **4**,105 (1963).

Sarkany, J., and R. D. Gonzalez, "On the Use of the Dynamic Pulse Method to Measure Metal Surface Areas," *J. Catal.*, **76**, 75 (1982).

Sloot H. J., C. A. Smolders, W. P. M. van Swaaij, and G. F. Versteeg, "High-Temperature Membrane Reactor for Catalytic Gas-Solid Reactions," *AIChE J.*, **38**, 887 (1992).

Sun, Yi-Ming, and Soon-Jai Khang, "A Catalytic Membrane Reactor: Its Performance in Comparison with Other Types of Reactors," *Ind. Eng. Chem. Res.*, **29**, 232 (1990).

Taylor, G., "Dispersion of Soluble Material in Solvent Flowing Slowly Through a Tube," *Proc. Roy. Soc.*, **A219**, 186 (1953).

Vincent, M. J., and R. D. Gonzalez, "A Langmuir-Hinshelwood Model for a Hydrogen Transfer Mechanism in the Selective Hydrogenation of Acetylene Over a $Pd/\gamma\text{-}Al_2O_3$ Catalyst Prepared by the Sol-Gel Method," *Appl. Catal. A*, **217**, 143 (2001).

Weirauch, W., "CMAI Conference Petrochemical Outlook," *Hydrol. Processes, Int. Ed.*, **79**, 19 (2000).

Wilke, C.R., "Diffusional Properties of Multicomponent Gases," *Chem. Eng. Progr.*, **46**, 95 (1950).

Yoldas, B. E., "Transparent Porous Alumina," *Amer. Ceram. Soc. Bull.*, **54**, 129 (1975).

Manuscript received May 24, 2001, and revision received Oct. 15, 2001.